Proceedings of the
47th IEEE Conference on Decision and Control
Cancun, Mexico, Dec. 9-11, 2008

Robust PI control of hysteretic systems

Sina Valadkhan, Kirsten Morris, and Amir Khajepour

Abstract— **Stability, tracking and the trajectories of a class of hysteretic systems controlled by a PI controller is considered. The system output (not its derivative) is measured and controlled. Only a simple bound on the controller gain parameter is assumed. The closed-loop system is BIBO-stable with a finite gain of one. Furthermore, provided that the desired output is within the limits of the system output, the system will track a constant reference input with zero steady-state error. A bound on the time required to achieve a specified error is obtained.**

I. Introduction

Hysteretic systems are seen in many applications. Smart materials, such as piezoceramics, shape-memory alloys and magnetostrictive materials, are an important group of hysteretic systems. Uncertainties seen in the physical system together with complex nonlinear behaviour of the system make it difficult to provide a robustly stabilizing controller for a hysteretic system.

A popular approach for control of a hysteretic system is to linearize the system by incorporating the inverse of the hysteresis, and then design a linear controller for the resulting linear system that is close to unity [1]–[3, e.g.]. In this approach, the model must of course be invertible. Furthermore, an accurate model of the hysteretic system is required since modelling errors will affect the overall performance and could lead to instability. Even small errors in the model can lead to quite large errors in the inverse model. Also, the inclusion of the inverse of the hysteresis model in the controller leads to a complex controller.

In [4], a magnetostrictive actuator is controlled by a hybrid optimal controller. The actuator input is computed by a hysteresis model offline. A PI controller is added to compensate for unmodeled dynamics and other errors.

For a passive hysteretic system, the stability of the controlled system can be established using the passivity theorem. The passivity of the Preisach model [5], [6], commonly used for smart materials, is shown in [7]. The system output is the time-derivative of the Preisach model output. In [8], a physics-based argument is used to prove the passivity of a magnetostrictive actuator. In this proof, no specific model is used and the results apply to any hysteresis model for magnetostrictive actuators. Passivity has been used to establish L_2-stability of velocity controllers for smart-material based actuators in [7] and [9].

Sina Valadkhan and Amir Khajepour are with the Department of Mechanical Engineering, University of Waterloo, Waterloo, Ontario, Canada, N2L 3G1 (svaladkh@uwaterloo.ca, akhajepour@uwaterloo.ca). Kirsten Morris is with the Department of Applied Mathematics, University of Waterloo, Waterloo, Ontario, Canada, N2L 3G1, (kmorris@uwaterloo.ca).

This research was supported by NSERC through the Idea to Innovation Program.

However, for many applications the position, not the velocity, is measured and controlled. In particular, position tracking is a common objective of many control systems. One example is a scanning microscope. The microscope tip is driven by a smart-material based actuator. The tip must move to a specified location.

In [10], [11], closed-loop control of hysteretic systems is studied using techniques for nonlinear dynamical systems. There is a common set of assumptions that the hysteretic system must satisfy, but different control system configurations are studied. In [10], pure integral control with a time-varying gain is studied, with additional dynamics included in the loop. Only constant inputs are considered. It is shown that the system is well-posed and that, if certain conditions are satisfied, the steady-state tracking error is zero. In [11], PID control of a second-order system that includes a hysteretic component is studied. Under certain conditions, it is shown that the system asymptotically tracks a constant input. One key assumption in these results is that the system has monotonic input/output behaviour.

In this work, the system is assumed to satisfy certain assumptions, one of which is related to monotonicity. The assumptions used are simpler than those used in [10], [11]. The Preisach model [6] is one of the most important hysteresis models in the literature. This model is frequently used for many smart materials [12]–[16]. In general, Preisach models satisfy the assumptions used here.

The system output, not its derivative, is measured and controlled. We are concerned with obtaining a controller with reasonable gains that can be implemented experimentally. A PI controller was chosen because of its availability and simplicity. For arbitrary reference signals, the closed-loop system is bounded-input-bounded-output (BIBO) stable with a finite gain of one. It is shown that the absolute value of the error decreases monotonically for a constant reference signal. In this case, provided that the desired output is within the limits of the system output, zero steady-state error is guaranteed. A bound on the time required to achieve a specified error is obtained. The results apply to a wide class of hysteretic systems and only a simple bound on the controller parameters is required. The results imply robust position control, even if errors in the model exist. Unlike the results presented in [10], [11], variable reference inputs are considered and BIBO stability with a finite gain is proven. In addition, more details about the trajectories of the closed-loop system for a constant input are given. Saturation is generally considered to be a destabilizing influence on a controlled system. However, in this approach, it is shown to assist stability. An expanded version of the work discussed

978-1-4244-3124-3/08/$25.00 ©2008 IEEE

in this paper can be found in [17].

In the next section, definitions and the framework used in this paper are established. BIBO stability of the closed-loop system is shown in Section 3. Section 4 is concerned with tracking of a constant input using a PI controller. In Section 5, the theory in the preceding sections is used to implement position control for a magnetostrictive actuator.

II. Framework

Define $\mathbb{R}_+$ to be the set of non-negative real numbers. For any interval $I \subset \mathbb{R}_+$, let $Map(I)$ indicate the set of real-valued functions defined on I. For $T > 0$ in some interval I, the truncation of $f \in Map(I)$ to the interval $[0, T]$ is

$$f_T(t) = \begin{cases} f(t), & 0 \le t \le T, \\ 0, & T < t. \end{cases}$$

Define $\mathcal{C}(I)$ to be the set of continous functions on an interval I. The norm of a function f in $\mathcal{C}(I)$ is

$$\|f\|_\infty = \sup_{t \in I} |f(t)| .$$

Definition 1: [5] An operator $\Gamma : Map(\mathbb{R}_+) \to Map(\mathbb{R}_+)$ has the *Volterra property* if, for any $v, w \in Map(\mathbb{R}_+)$ and any non-negative T, $v_T = w_T$ implies that $(\Gamma v)_T = (\Gamma w)_T$.

Definition 2: [18] An operator $\Gamma : Map(\mathbb{R}_+) \to Map(\mathbb{R}_+)$ is *rate independent* if

$$(\Gamma v) \circ \varphi = \Gamma(v \circ \varphi)$$

for all $v \in Map(\mathbb{R}_+)$ and all continuous monotone time transformations $\varphi : \mathbb{R}_+ \to \mathbb{R}_+$ satisfying $\varphi(0) = 0$ and $\lim_{t \to \infty} \varphi(t) = \infty$.

Definition 3: [18] An operator $\Gamma : Map(\mathbb{R}_+) \to Map(\mathbb{R}_+)$ is a *hysteresis operator* if it is rate independent and has the Volterra property.

The Volterra property states that the hysteretic system output does not depend on future inputs; that is, determinism. A deterministic, rate independent operator is a hysteresis operator.

For any $\delta > 0$, $0 \le t_1 < t_2$, and any $w \in \mathcal{C}([0, t_1])$ define

$$B_1(w, t_1, t_2) := \{u \in \mathcal{C}([0, t_2]) |\ u_{t_1} = w_{t_1}\} \quad (1)$$

$$B_2(w, t_1, t_2, \delta) := \{u \in \mathcal{C}([0, t_2]) |\ u_{t_1} = w_{t_1}, \ \max_{t_1 \le \tau \le t_2} |u(\tau) - w(t_1)| < \delta\}. \quad (2)$$

Denote the hysteresis model input and output by u and y, respectively. The following assumptions on the system are used in this paper.

(A1) If $u(t)$ is continuous then $y(t)$ is continuous. That is, $\Gamma : \mathcal{C}(I) \to \mathcal{C}(I)$ where I is the interval of interest.

(A2) (Lipshitz property) There exists $\lambda > 0$ such that for every interval $[t_1, t_2]$ where $0 \le t_1 < t_2$ and every $w \in \mathcal{C}([0, t_1])$, the following inequality holds for all $u_1, u_2 \in B_1(w, t_1, t_2)$.

$$\sup_{t_1 \le \tau \le t_2} |\Gamma(u_1)(\tau) - \Gamma(u_2)(\tau)| \le \lambda \sup_{t_1 \le \tau \le t_2} |u_1(\tau) - u_2(\tau)|. \quad (3)$$

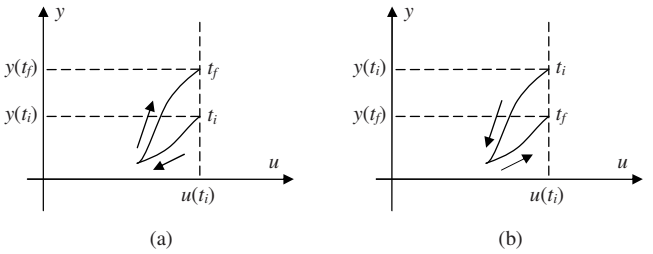

Fig. 1. (a) A clockwise hysteresis loop, and (b) a counter-clockwise hysteresis loop.

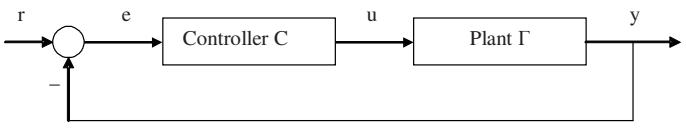

Fig. 2. The closed-loop system.

(Note by definition of $B_1(w, t_1, t_2)$ and $B_2(w, t_1, t_2, \delta)$, the Volterra property implies that $\Gamma(u_1)(\tau) = \Gamma(u_2)(\tau)$ for $0 \le \tau \le t_1$.)

(A3) Consider an arbitrary interval $[t_i, t_f]$. If for every $t \in [t_i, t_f]$, $u(t_i) \ge u(t)$, then $y(t_i) \ge y(t_f)$. Alternatively, if for every $t \in [t_i, t_f]$, $u(t_i) \le u(t)$, then $y(t_i) \le y(t_f)$.

(A4) (saturation) There exists some $u_{sat} > 0$, y_+ and y_- such that if $u(t) \ge u_{sat}$ then $(\Gamma u)(t) = y_+$ and $(\Gamma(-u))(t) = y_-$.

There is a close connection between assumption (A3) and monotonicity of the hysteretic system, in a sense that an increasing input results in increasing output and the same for decreasing inputs/outputs. By setting $t = t_f$, it is seen that if assumption (A3) holds, the hysteretic system is monotonic. The converse is not true. In Figure 1(a), a hysteretic system with a clockwise hysteresis loop is shown. This plant is monotonic, but does not satisfy assumption (A3). In Figure 1(b), a plant with a counter-clockwise hysteresis loop is shown. The plant is monotonic and assumption (A3) is satisfied.

Many standard hysteretic systems satisfy these assumptions. The main restriction in our framework is the restriction to hysteresis operators (Definition 3). In particular, the commonly used Preisach model [5], [6] satisfies the assumptions for any practical system [17].

III. Stability of the closed-loop system

In this section, the trajectories of the solutions for the closed-loop system are examined. It is shown that the system is bounded-input-bounded-output (BIBO)-stable.

Definition 4: A mapping $R : \mathcal{C}(I) \to \mathcal{C}(I)$ is BIBO-stable if for every $u \in \mathcal{C}(I)$, $Ru \in \mathcal{C}(I)$ and there exists a finite constant ρ such that

$$\|(Ru)(t)\|_\infty \le \rho \|u\|_\infty, \ \forall u \in \mathcal{C}(I) \quad (4)$$

The smallest such constant ρ is the gain.

Consider the closed-loop feedback system shown in Figure 2, where the plant is represented by a hysteresis model Γ.

The following PI controller is used for position control:

$$\hat{C}(s) = \frac{K_I}{s} + K_P \tag{5}$$

where K_I and K_P are constants. The controller parameters are assumed only to satisfy

(B1) For the controller in (5), $0 \leq K_P\lambda < 1$ and $K_I > 0$ where $\lambda > 0$ is the Lipchitz constant in assumption (A2).

The following additional assumption on the reference input is used.

(B2) The reference signal $r(t)$ is a continuous function of time; that is, $r(t) \in \mathcal{C}(I)$ where I is the interval of interest.

The closed-loop system shown in Figure 2 is described by the following equations:

$$\begin{aligned} e(t) &= r(t) - y(t), & (6)\\ f(t) &= \int_0^t e(\tau)d\tau, & (7)\\ u(t) &= K_P e(t) + K_I f(t), & (8)\\ y(t) &= \Gamma\left[u(\cdot)\right](t). & (9) \end{aligned}$$

The only assumptions on the system required to show existence of a unique continuous solution are (A1) and (A2).

Theorem 5: [17] Assume that (A1), (A2), (B1), and (B2) hold. Then (6-9) have a unique solution for $u \in \mathcal{C}([0,\infty))$ and $y \in \mathcal{C}([0,\infty))$.

The following theorem establishes BIBO-stability of the closed loop. Furthermore, the system possesses unity gain for any choice of controller parameters.

Theorem 6: [17] Assume that the closed-loop system has a unique solution for $u, y \in \mathcal{C}([0,\infty))$ and assumptions (A3), (B1), and (B2) hold. Furthermore, assume that $u(0) = 0$. If $|y(0)| \leq \|r\|_\infty$, then $\|y\|_\infty \leq \|r\|_\infty$. That is, the closed loop system is BIBO-stable with gain 1.

For hysteretic systems satisfying the saturation assumption (A4), boundedness of the output can be derived from saturation. Theorem 6 extends this result to hysteretic systems that do not satisfy the saturation assumption. Whether or not saturation is present, the closed-loop system has a gain of 1.

IV. Tracking

In this section we show that PI controllers provide a closed loop system that tracks a constant input with zero steady-state error and no overshoot. A bound on the time required to achieve a specified error is obtained.

The following result guarantees that the tracking error decreases monotonically.

Theorem 7: Assume that r is a constant in some interval $[t_0, T]$, the closed-loop system has a unique solution for $u, y \in \mathcal{C}([0,T])$, and assumptions (A3) and (B1) hold. If for some nonnegative ρ, $|r - y(t_0)| \leq \rho$, then $|r - y(t_1)| \leq \rho$ for all $t_0 \leq t_1 \leq T$.

Proof: Assume that for some t_1, $r - y(t_1) < -\rho$. For $r - y(t_1) > \rho$, the proof is similar.

$$e(t_1) < -\rho. \tag{10}$$

Define $t_{\max u}$ to be the time at which $u(t)$ is maximized on $[t_0, t_1]$:

$$u(t_{\max u}) \geq u(t), \forall t \in [t_0, t_1]. \tag{11}$$

Define $t_{\max f}$ to be the time at which $f(t)$ is maximized on $[t_0, t_1]$:

$$f(t_{\max f}) \geq f(t), \forall t \in [t_0, t_1].$$

Since the plant output $y(t)$ is continuous, $f(t)$ is continuously differentiable. Inequality (10) implies that $\dot{f}(t_1) = e(t_1) < 0$, and so $f(t)$ is strictly decreasing in the vicinity of t_1. This implies that

$$t_{\max f} \neq t_1.$$

If $t_{\max f} \neq t_0$, maximization of $f(t)$ at $t_{\max f}$ implies that $\dot{f}(t_{\max f}) = 0$, or,

$$e(t_{\max f}) = 0, \text{ if } t_{\max f} \neq t_0. \tag{12}$$

By definition of $t_{\max f}$ and $t_{\max u}$,

$$\begin{aligned} u(t_{\max f}) &\leq u(t_{\max u}), & (13)\\ f(t_{\max f}) &\geq f(t_{\max u}). & (14) \end{aligned}$$

Using (8) and (13)

$$K_P e(t_{\max f}) + K_I f(t_{\max f}) \leq K_P e(t_{\max u}) + K_I f(t_{\max u}).$$

But inequality (14) implies that

$$K_P e(t_{\max f}) \leq K_P e(t_{\max u}). \tag{15}$$

Using assumption (A3) and (11) we obtain that

$$y(t_{\max u}) \geq y(t_1),$$

and so,

$$e(t_{\max u}) \leq e(t_1). \tag{16}$$

Case 1: $K_P > 0$

By combining (10), (15), and (16) we have

$$e(t_{\max f}) < -\rho \leq 0. \tag{17}$$

Since $e(t_{\max f}) \neq 0$, (12) implies that $t_{\max f} = t_0$. Rewriting inequality (17) leads to

$$e(t_0) = r - y(t_0) < -\rho$$

as required.

Case 2: $K_P = 0$

Equation (8) simplifies to

$$u(t) = K_I f(t).$$

Since $K_I > 0$, any choice for $t_{\max u}$ is also a choice for $t_{\max f}$. At $t_{\max f}$, $u(t)$ is maximized. By repeating the argument above for (16) we obtain that

$$e(t_{\max f}) \leq e(t_1).$$

Using inequality (10) leads to

$$e(t_{\max f}) < -\rho \leq 0.$$

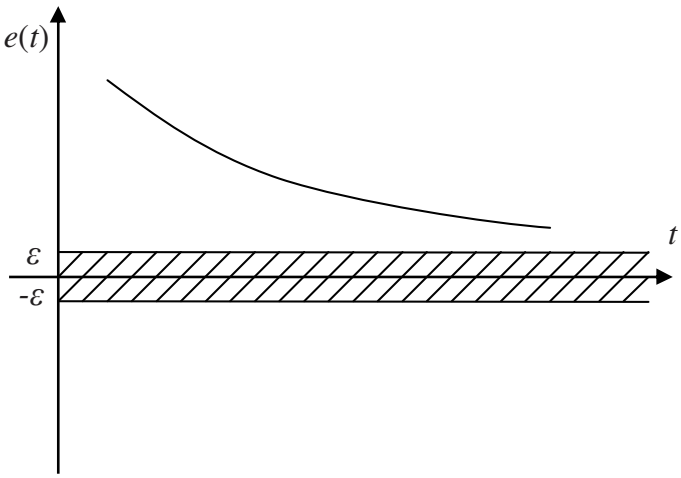

Fig. 3. The error $e(t)$ versus time.

Similar to the previous case, $e(t_{\max f}) \neq 0$ and (12) imply that $t_{\max f} = t_0$ and so

$$e(t_0) = r - y(t_0) < -\rho.$$

The proof is complete. ■

Theorem 7 states that during a period where the input is constant, the absolute value of the error is never increased. As a result, an oscillatory response or an overshoot cannot be seen. The following theorem proves that, if in addition to the assumptions of the previous theorem, the saturation assumption (A4) holds, then the error can be made arbitrarily small.

Theorem 8: Let t_0 be a non-negative real number. Assume that $r(t)$ is a constant, r, in $[t_0, \infty)$, the closed-loop system has a unique solution for $u, y \in \mathcal{C}([0, \infty))$, and that assumptions (A3), (A4), and (B1) hold. If $y_- \leq r \leq y_+$, then for every $\varepsilon > 0$,

$$|r - y(t)| \leq \varepsilon, \forall t \geq \bar{t} + t_0,$$

where

$$\bar{t} = \frac{\frac{u_{sat}}{K_I} + |f(t_0)|}{\varepsilon}. \tag{18}$$

Consequently, $\lim_{t\to\infty} y(t) = r$.

Proof: Assume that for some ε and $t \geq \bar{t}+t_0$, $r-y(t) > \varepsilon$. The proof for the case $y(t) - r > \varepsilon$ is identical.

Theorem 7 implies that for all $t' \in [t_0, t]$,

$$|r - y(t')| = |e(t')| > \varepsilon. \tag{19}$$

As illustrated in Figure 3, since $e(t) > 0$ and $e(\cdot)$ is continuous, $e(t') > 0$. Integrating (19) from t_0 to $t_0 + \bar{t}$, we have

$$\int_{t_0}^{t_0+\bar{t}} e(t')dt' \geq \varepsilon\bar{t}.$$

Using the definition of f, (7), it follows that

$$f(t_0 + \bar{t}) \geq f(t_0) + \varepsilon\bar{t}. \tag{20}$$

Since $\bar{t}$ is defined by (18),

$$\varepsilon\bar{t} \geq \frac{u_{sat}}{K_I} - f(t_0). \tag{21}$$

Substituting this into (20) leads to

$$f(t_0 + \bar{t}) \geq \frac{u_{sat}}{K_I}.$$

Since $t \geq \bar{t} + t_0$, (19) implies that

$$e(t_0 + \bar{t}) > \varepsilon. \tag{22}$$

By using equation (8), a bound on $u(t_0+\bar{t})$ can be obtained:

$$u(t_0 + \bar{t}) \geq K_P\varepsilon + u_{sat} \geq u_{sat}.$$

Using assumption (A4), $y(t_0 + \bar{t}) = y_+$. From (22),

$$r > y_+.$$

Thus, if $r - y(t) > \varepsilon$ for some $t \geq \bar{t}+t_0$, $r > y_+$. Similarly, if $y(t) - r > \varepsilon$, then $r < y_-$. Hence, $y_- \leq r \leq y_+$ implies that $|r - y(t)| \leq \varepsilon$ for all $t \geq \bar{t} + t_0$ as was to be shown.

It was shown that for every $\varepsilon > 0$, there is a $\bar{t}$ such that $|r - y(t)| \leq \varepsilon$ for all $t \geq \bar{t} + t_0$. This is the definition of limit. Thus, $\lim_{t\to\infty} y(t) = r$. ■

Theorem 8 gives an upper limit for the time required to achieve any accuracy ε. The condition $y_- \leq r \leq y_+$ is just that the desired reference point is within the saturation limits. The above theorem states that if the input to the closed loop is within the saturation limits, zero steady-state error is guaranteed.

Theorem 6 can be used to design a controller for position control. The controller must only satisfy assumptions $0 \leq \lambda K_P < 1$ and $K_I > 0$. In the next section, a position controller is designed and evaluated experimentally.

V. Experimental results

In the previous sections, tracking and stability for position control of hysteretic systems were shown for a PI controller. In this section, these results are used to develop a stabilizing position controller for a magnetostrictive actuator.

To evaluate the position controller experimentally, a magnetostrictive actuator is used. In this actuator, a rod made of Terfenol-D, a magnetostrictive material, provides actuation. This material reacts to a magnetic field. In the presence of a magnetic field, this material generates a small mechanical displacement. The displacement is measured by an optical encoder with a resolution of $10nm$.

To provide the requested magnetic field, the Terfenol-D rod is used inside an electrical magnet. The magnet is powered by a programmable electrical current source. The current source is controlled by a PC computer. Several sensors are included in the actuator to measure flux density and temperature. Details and a photograph of the apparatus are in [12]. The sensors' measurements are sent to the PC computer. MATLAB Real-Time Workshop® is used with the PC computer. The controller is implemented within MATLAB.

Terfenol-D cannot withstand tension and should be in compression for proper operation. The compression is provided by a set of washer springs. The springs are soft enough that it can be assumed that the compression force is constant when the Terfenol-D rod changes size. The force of the springs can be adjusted. The force is measured by a load cell.

For a magnetostrictive material, magnetic field H and magnetization M are the input and output, respectively. The relation between magnetic field H and magnetization M can be represented by a Preisach model with a positive weight function with compact support [12]. Assumptions (A1)-(A4) are satisfied.

In most applications, it is desired to control the displacement λ produced by the actuator. The following equation relates magnetization M to displacement [12], [19]:

$$\lambda = \gamma_1 M^2 + \gamma_2 M^4 \tag{23}$$

where γ_1 and γ_2 are constants at a constant mechanical load. Using this relation, position control is achieved by controlling the magnetization M.

To find the magnetization in the magnetostrictive actuator, the displacement produced is measured and equation (23) is used to compute magnetization. The same relation is used to compute the desired magnetization and hence, errors in (23) do not affect the closed-loop performance.

Theorem 6 states that any PI controller satisfying assumption (B1) provides stability. To find the optimal gains for the controller, a performance criteria is needed. Here, tracking performance is used; that is, an optimal set of controller parameters should minimize the cost function

$$J = \int_{t_1}^{t_2} (y - r)^2 dt,$$

where r is the reference input, y is the closed-loop output and $[t_1, t_2]$ is the time range of interest, subject to the parameter constraints (B1). A smaller value of J means a closer match between the actual and desired outputs.

Because of the nonlinear and complex structure of the system, the only method for minimizing J is numerical optimization. For this purpose, the closed-loop is simulated by using a Preisach model with a general weight function. The model is identified in [12]. Using the Preisach model, y is computed as a function of controller parameters. The cost function J is numerically minimized using Nelder-Mead simplex direct search method [20] with a reference signal r chosen as a series of step inputs. Formally, the ideal version of such a reference input is not continuous. However, in experiment there is a rapid but continuous change between values and so the signal is continuous. (Furthermore, due to the nature of a hysteresis operator, there is no difference between the output of a hysteretic system with a step discontinuity and one with a smooth monotonic change between the same values [5].)

The optimum values for the controller gains are: $K_I = 38.02 s^{-1}$ and $K_P = 0.0785$. The optimal gains were tested experimentally for different reference signals.

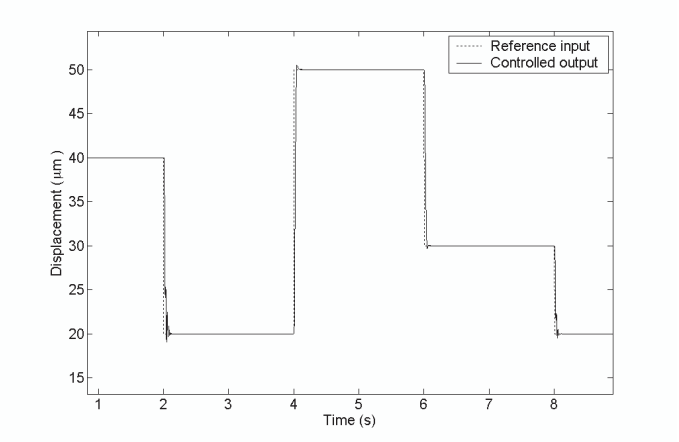

Fig. 4. The closed-loop response to various steps.

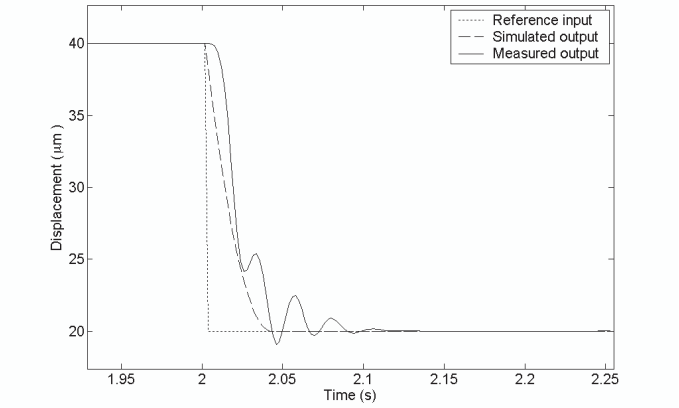

Fig. 5. Transient response after a step. The effects of a moving mass are seen.

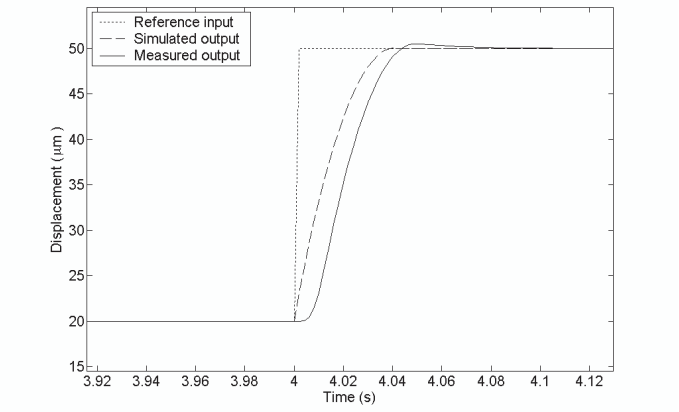

Fig. 6. Transient response after a step. No vibration is seen.

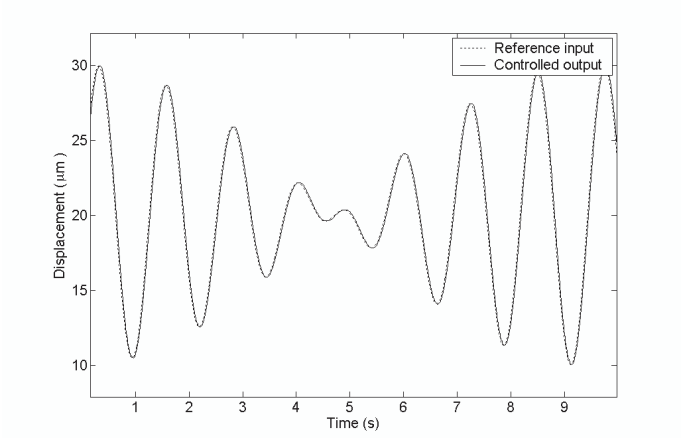

Fig. 7. Tracking response of the closed loop.

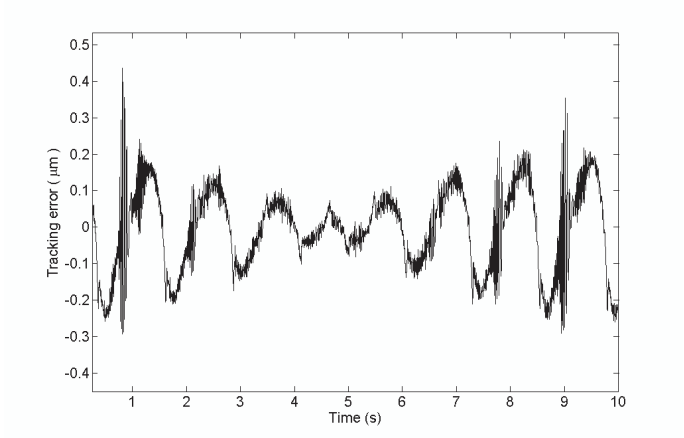

Fig. 8. Tracking error of the closed loop.

In Figure 4, the closed-loop response of the system to step input is shown for the optimized controller. Excellent tracking is seen. As predicted by Theorem 8, there is no steady-state error. In Figures 5 and 6, portions of the response are magnified. The nonlinear nature of the system exhibits different responses in different conditions. The system settles to $\pm 10nm$ of the reference signal in $0.175s$ and $0.122s$ in Figures 5 and 6, respectively. This is within the accuracy of the sensor used. A small overshoot is seen in Figures 5 and 6. In Figure 5, some oscillations are also observed. Theorem 7 implies that there is no oscillatory response or overshoot. The overshoots and oscillations are likely caused by some unmodeled mass in the system. Simulation results are also shown in Figures 5 and 6. Since unmodeled dynamics are not present in the simulation, no overshoot or vibrations are seen. This is consistent with the results of Theorem 7.

In Figure 7, the system response to a sinusoidal input with varying amplitude is displayed. In the previous sections, it was shown that the closed-loop system is BIBO-stable for variable reference signals. Stability is observed and the reference trajectory is followed accurately. In Figure 8, the tracking error for the same experiment is shown. The root-mean-square tracking error is $0.11\mu m$, a relative error of 1.1%.

REFERENCES

[1] X. Tan and J. S. Baras, "Modeling and control of hysteresis in magnetostrictive actuators," *Automatica*, vol. 40, no. 9, September 2004, pp. 1469-1480.

[2] J. M. Nealis and R. C. Smith, "Model-based robust control design for magnetostrictive transducers operating in hysteretic and nonlinear regimes," *IEEE transactions on control systems technology*, vol. 15, no. 1, January 2007, pp. 22-39.

[3] ——, "Robust control of a magnetostrictive actuator," *Proceedings of SPIE, the international society for optical engineering*, vol. 5049, 2003, pp. 221-232.

[4] W. S. Oates and R. C. Smith, "Nonlinear perturbation control for magnetic transducers," *Proceedings of the 45th IEEE conference on decision and control*, 2006, pp. 2441-6.

[5] M. Brokate and J. Sprekels, *Hysteresis and phase transitions*. New York: Springer, 1996.

[6] I. Mayergoyz, *Mathematical models of hysteresis and their applications*. Amsterdam, Boston: Elsevier Academic Press, 2003.

[7] R. B. Gorbet, K. A. Morris, and D. W. L. Wang, "Passivity-based stability and control of hysteresis in smart actuators," *IEEE transactions on control systems technology*, vol. 9, no. 1, January 2001, pp. 5-16.

[8] S. Valadkhan, K. A. Morris, and A. Khajepour, "Passivity of magnetostrictive materials," *SIAM Journal of applied mathematics*, vol. 67, No. 3, 2007, pp. 667-686.

[9] ——, "Robust control of smart material-based actuators," in *New Frontiers in Control Theory and Applications*, V. B. andS. Boyd and H. Kimura, Eds. Springer-Verlag, 2008.

[10] H. Logemann, E. P. Ryan, and I. Shvartsman, "Integral control of infinite-dimensional systems in the presence of hysteresis: an input-output approach," *ESAIM - control, optimisation and calculus of variations*, to appear.

[11] B. Jayawardhana, H. Logemann, and E. P. Ryan, "PID control of second-order systems with hysteresis," *preprint*.

[12] S. Valadkhan, K. A. Morris, and A. Khajepour, "A review and comparison of hysteresis models for magnetostrictive materials," *Journal of intelligent material systems and structures*, to appear.

[13] R. B. Gorbet, D. W. L. Wang, and K. A. Morris, "Preisach model identification of a two-wire SMA actuator," *Proceedings, IEEE international conference on robotics and automation*, vol. 3, 1998, pp. 2161-7.

[14] D. Hughes and J. T. Wen, "Preisach modeling of piezoceramic and shape memory alloy hysteresis," *Smart materials and structures*, vol. 6, 1997, pp. 287-300.

[15] S. B. Choi and Y. M. Han, "Hysteretic behavior of a magnetorheological fluid: experimental identification," *Acta mechanica*, vol. 180, No. 1-4, 2005, pp. 37-47.

[16] X. Zhou, J. Zhao, G. Song, and J. D. Abreu-Garcia, "Preisach modeling of hysteresis and tracking control of a Thunder actuator system," *Proceedings of SPIE - the international society for optical engineering*, vol. 5049, 2003, pp. 112-125.

[17] S. Valadkhan, K. A. Morris, and A. Khajepour, "Stability and robust position control of hysteretic systems," *Int'l J. of Robust and Nonlinear Control*, submitted.

[18] M. Brokate, "Hysteresis operators," *in Phase transitions and hysteresis*, edited by A. Visintin, Springer-Verlag, Berlin, 1994, pp. 1-38.

[19] D. C. Jiles, "Theory of the magnetomechanical effect," *Journal of physics D: applied physics*, vol. 28, no. 8, 14 August 1995, pp. 1537-1546.

[20] D. P. Bertsekas, *Nonlinear Programming*. Belmont, Massachusetts: Athena Scientific, 1999.